MECSOL 2019 - Proceedings of the 7th International Symposium on Solid Mechanics,
V. Tita, A. Ferreira, M.L. Ribeiro, A. Vieira and A.T. Beck (Editors), ABCM, Sao Carlos, SP, Brazil, April 15th to 17th, 2019

A CONSISTENT TIMOSHENKO ELEMENT BEAM FOR SMALL STRAIN BUT LARGE ROTATION

Eliseu Lucena Neto, Adriano Carvalho Neto, Francisco Monteiro, and Rodrigo Santos

Instituto Tecnológico de Aeronáutica, 12228-900, São José dos Campos, SP, Brazil

Abstract: A finite element for plane frames under small strains but large rotations, based on the total Lagrangian description, is developed. The element stems from the Timoshenko beam theory with linear approximations for axial and transverse displacements as well as for the rotation. In addition to identify analytical and numerically the membrane and transverse shear lockings, it is shown how to properly alleviate them.

Keywords: Timoshenko beam, finite element, membrane locking, shear locking, Total Lagrangian description

INTRODUCTION

Figure 1 shows the general motion of a cantilever beam which is, for description purpose, imagined as being an assemblage of four finite elements and subjected to a moment load at the free end. In order to determine the unknown current equilibrium configuration C_n, when the magnitude of the applied moment is M_n, one employs a nonlinear iterative procedure which departs from the successive knowledge of the previous configurations C_0, …, C_i, …, C_{n-1} to estimate the actual configuration. If the current equilibrium is described taking as reference just one of the previous known configurations, then one says that a Lagrangian formulation is settled. The total, generalized and updated Lagrangian descriptions draw the element movement assuming as reference the configurations C_0, C_i and C_{n-1}, respectively (Cescotto et al., 1979).

There are some applications, such as in civil, marine and aerospace engineering, in which structural beams experience large rotations and displacements whereas the strains remain small. The assumption of small strains is quite realistic for civil engineering design, since they must satisfy building code requirements. Unfortunately, such an assumption does not simplify the problem when rotations are not small because the problem can be yet strongly nonlinear. However, it allows the use of traditional linear constitutive equations, even for large rotations, provided the second Piola-Kirchhoff stress tensor be related to the Green strain tensor since they are unaffected by rigid-body motion (Bathe, 1996, Belytschko et al., 2014). In comparison with the classical Euler–Bernoulli beam theory, the Timoshenko theory has been proved a popular choice to deal with highly complex nonlinearities of beams leading to simple displacement strain relations.

Aiming to demonstrate the possibilities of the application of Timoshenko beam theory, Adámek (2018) presents and discusses some problems for three-layered elastic beams with symmetric composition. In particular, the equivalent single layer theory varying the shear correction factor is focused. In the context of strain gradient elasticity, Balobanov and Niiranen (2018) formulate a Timoshenko beam element for both static and dynamic analysis. A model comparison between Timoshenko and Euler–Bernoulli beam models has proved the relevance of the former by means of experimental results on nano-beams. Kaya and Dowling (2016) establish a Timoshenko beam based estimation method to assess the unknown structural response of multi-story buildings.

In a finite element framework, it is well understood that the usual linear approximations for axial and transverse displacements as for the rotation, assumed in Timoshenko-type beam elements, can lead to numerical ill-conditioning resulting in membrane and shear locking phenomena. Such lockings have been overcome by several methods including selective reduced integration, mixed formulations, among others (Zhang et al., 2018).

A brief review of the literature has shown that the beam analysis for arbitrary large displacement gradients is still an open problem (Beheshti, 2016). The present article consistently incorporates small strains into a total Lagrangian formulation to formulate a finite element for plane frames. The element stems from the Timoshenko beam theory with linear approximations for axial and transverse displacements as well as for the rotation. Although none numerical results have been disclosed, Felippa (2014) provides an excellent discussion about the theoretical aspects of this finite element formulation. In addition to identify analytical and numerically the membrane and transverse shear lockings, it is

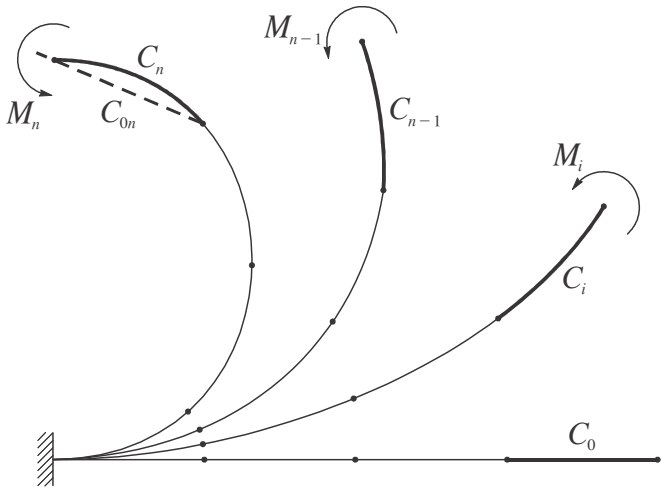

Figure 1 – Equilibrium configurations.

shown how to properly alleviate them. By providing consistent strain-gradient-based finite elements, it is expected that the proposed element may find practical use.

FUNDAMENTALS

Consider a section of a beam shown in Fig. 2. Due to the deformation, a point at $B(X,Y,Z)$ in the initial configuration moves to $b(x,y,z)$ in the current configuration. Under the kinematic assumptions of the Timoshenko beam formulation, the location of any (particle) point on the beam can be found through the map

$$\begin{Bmatrix} x \\ y \\ z \end{Bmatrix} = \begin{Bmatrix} u \\ 0 \\ w \end{Bmatrix} + \begin{bmatrix} 1 & 0 & \sin\theta \\ 0 & 1 & 0 \\ 0 & 0 & \cos\theta \end{bmatrix} \begin{Bmatrix} X \\ Y \\ Z \end{Bmatrix} \tag{1}$$

where $u(X)$, $w(X)$ are the displacements of the point $A(X,Y,Z)$ on the undeformed beam axis, in the XZ system, and $\theta(X)$ represents the rotation of the beam cross-section.

The deformation gradient matrix

$$\mathbf{F} = \begin{bmatrix} \partial x/\partial X & \partial x/\partial Y & \partial x/\partial Z \\ \partial y/\partial X & \partial y/\partial Y & \partial y/\partial Z \\ \partial z/\partial X & \partial z/\partial Y & \partial z/\partial Z \end{bmatrix} = \begin{bmatrix} 1+u'+Z\theta'\cos\theta & 0 & \sin\theta \\ 0 & 1 & 0 \\ w'-Z\theta'\sin\theta & 0 & \cos\theta \end{bmatrix} \tag{2}$$

can be decomposed into

$$\mathbf{F} = \begin{bmatrix} 1+u' & 0 & 0 \\ 0 & 1 & 0 \\ w' & 0 & 0 \end{bmatrix} + \begin{bmatrix} \cos\theta & 0 & \sin\theta \\ 0 & 1 & 0 \\ -\sin\theta & 0 & \cos\theta \end{bmatrix} \begin{bmatrix} Z\theta' & 0 & 0 \\ 0 & 1 & 0 \\ 0 & 0 & 1 \end{bmatrix} = \mathbf{F}_0 + \mathbf{R}\mathbf{F}_1 \tag{3}$$

where primes denote derivatives with respect to X. Since $\mathbf{R}$ is an orthogonal tensor,

$$\mathbf{F} = \mathbf{R}(\mathbf{R}^T\mathbf{F}_0 + \mathbf{F}_1) = \mathbf{R}\mathbf{F}_2 \tag{4}$$

The tensor $\mathbf{F}_2$ represents the deformational part of $\mathbf{F}$ and it is associated with the movement of the beam cross-section between the (undeformed) rotated and current configurations. Because all displacement gradients provided by $\mathbf{F}_2$ are expected to have a small magnitude, the Green strain tensor $\mathbf{E}$, under the small strain assumption, can be linearized by

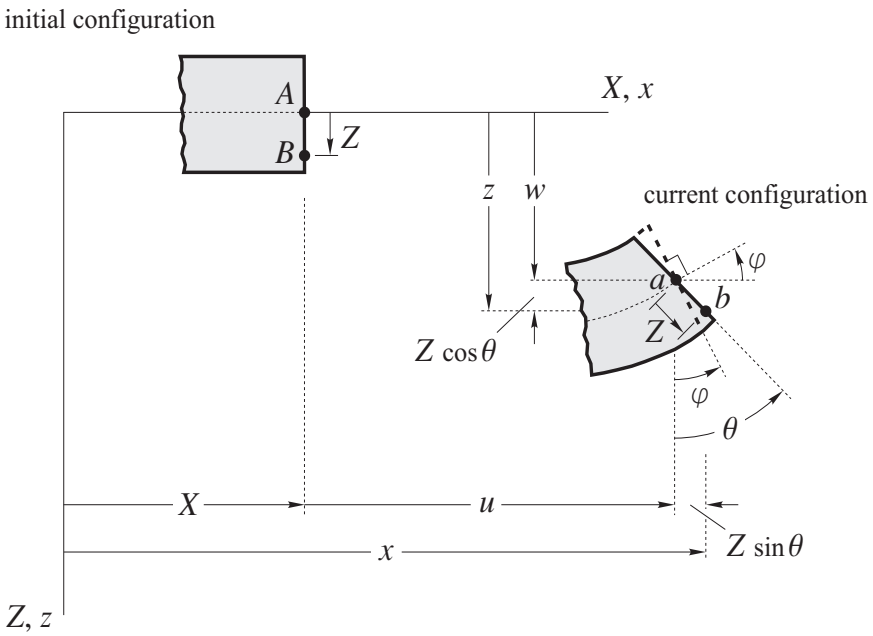

Figure 2 – Timoshenko beam kinematics.

$$\mathbf{E} = \frac{1}{2}(\overline{\mathbf{F}}^T\overline{\mathbf{F}} - \mathbf{I}) \approx \frac{1}{2}(\overline{\mathbf{F}} + \overline{\mathbf{F}}^T) - \mathbf{I} \tag{5}$$

It is easy to show that the previous simplification leads to

$$\mathbf{E} = \begin{bmatrix} e_0 + Z\kappa & 0 & \frac{1}{2}\gamma \\ 0 & 0 & 0 \\ \frac{1}{2}\gamma & 0 & 0 \end{bmatrix} = \begin{bmatrix} e_X & 0 & \frac{1}{2}\gamma_{XY} \\ 0 & 0 & 0 \\ \frac{1}{2}\gamma_{XY} & 0 & 0 \end{bmatrix} \tag{6}$$

where

$$\begin{Bmatrix} e_0 \\ \kappa \\ \gamma \end{Bmatrix} = \begin{Bmatrix} (1+u')\cos\theta - w'\sin\theta - 1 \\ \theta' \\ (1+u')\sin\theta + w'\cos\theta \end{Bmatrix} \tag{7}$$

are the generalized strains, and $u(X)$, $w(X)$, $\theta(X)$ are the displacement field variables.

FINITE ELEMENT

Figure 3 shows a 2D beam element with length L_e and cross-sectional area A, subjected to the distributed loads q_X, q_Y and the concentrated end forces F_{Xi}, F_{Zi}, M_{Yi} ($i = 1,2$). The element has two end nodes and three displacement fields $u(X)$, $w(X)$ and $\theta(X)$ to be interpolated.

The principal of virtual work states that

$$\delta W_i + \delta W_e = 0 \tag{8}$$

where

$$\delta W_i = -\iiint (S_X \delta e_X + S_{XY}\delta\gamma_{XY})\,dA\,dX \qquad \delta W_e = \int (q_X\delta u + q_z\delta w)dX + F_{Xi}\delta u_i + F_{Zi}\delta w_i + M_{Yi}\delta\theta_i \tag{9}$$

identifies the internal and external virtual work, respectively.

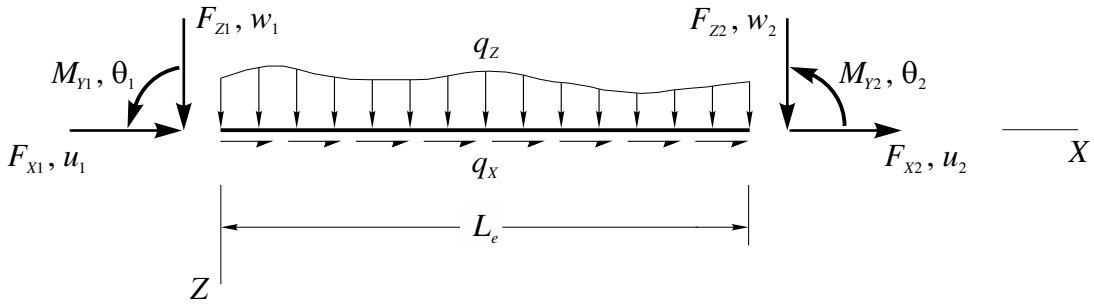

Figure 3 – Timoshenko beam element.

The second Piola-Kirchhoff stress tensor components S_X and S_{XY} are related with the Green strain components e_X and γ_{XY} through the constitutive equations

$$S_X = Ee_x \qquad S_{XY} = G\gamma_{XY} \tag{10}$$

The material is defined by the Young's modulus E and shear modulus G. Assuming that $\iint Z dA = 0$ and $\iint Z^2 dA = I$ then

$$\delta W_i = -\int (N\delta e_0 + M\delta\kappa + Q\delta\gamma) dX \tag{11}$$

where

$$N = \iint S_X dA = EAe_0 \qquad M = \iint ZS_X dA = EI\kappa \qquad Q = \iint S_{XY} dA = KGA\gamma \tag{12}$$

specify the generalized constitutive relationship. The symbol K stands for the shear correction factor (Reddy, 2004).

The element displacement field variables are approximated by

$$u = \mathbf{N}_u \cdot \mathbf{d} \qquad w = \mathbf{N}_w \cdot \mathbf{d} \qquad \theta = \mathbf{N}_\theta \cdot \mathbf{d} \tag{13}$$

where

$$\mathbf{d} = \lfloor u_1 \quad w_1 \quad \theta_1 \quad u_2 \quad w_2 \quad \theta_2 \rfloor^T \tag{14}$$

collects the nodal values of u, w and θ, and

$$\begin{aligned} \mathbf{N}_u &= \lfloor 1 - X/L_e \quad 0 \quad 0 \quad X/L_e \quad 0 \quad 0 \rfloor^T \\ \mathbf{N}_w &= \lfloor 0 \quad 1 - X/L_e \quad 0 \quad 0 \quad X/L_e \quad 0 \rfloor^T \\ \mathbf{N}_\theta &= \lfloor 0 \quad 0 \quad 1 - X/L_e \quad 0 \quad 0 \quad X/L_e \rfloor^T \end{aligned} \tag{15}$$

are the shape functions. Substitution of (13) into (8), taking into account (11) and (7), yields

$$\delta\mathbf{d}^T \left[-\mathbf{f}_N(\mathbf{d}) - \mathbf{f}_M(\mathbf{d}) - \mathbf{f}_Q(\mathbf{d}) + \int_0^{L_e} (q_X \mathbf{N}_u + q_Z \mathbf{N}_w) dx + \mathbf{f} \right] = \mathbf{0} \tag{16}$$

with

$$\mathbf{f}_N(\mathbf{d}) = \int_0^{L_e} N\{\cos\theta\,\mathbf{N}'_u - \sin\theta\,\mathbf{N}'_w - [(1+u')\sin\theta + w'\cos\theta]\mathbf{N}_\theta\}dX$$
$$\mathbf{f}_M(\mathbf{d}) = \int_0^{L_e} M\,\mathbf{N}'_\theta dX \tag{17}$$
$$\mathbf{f}_Q(\mathbf{d}) = \int_0^{L_e} Q\{\sin\theta\,\mathbf{N}'_u + \cos\theta\,\mathbf{N}'_w + [(1+u')\cos\theta - w'\sin\theta]\mathbf{N}_\theta\}dX$$

Since the components of $\delta\mathbf{d}$ are arbitrary and independent, the discretized version of the equilibrium problem is given by (Zeinkiewicz et al., 2013)

$$\boldsymbol{\Psi}(\mathbf{d}) = -\mathbf{f}_i(\mathbf{d}) + \mathbf{f}_e = -\left[\mathbf{f}_N(\mathbf{d}) + \mathbf{f}_M(\mathbf{d}) + \mathbf{f}_Q(\mathbf{d})\right] + \left[\int_0^{L_e} (q_X\mathbf{N}_u + q_Z\mathbf{N}_w)dx + \mathbf{f}\right] = \mathbf{0} \tag{18}$$

where the unbalanced force vector $\boldsymbol{\psi}$ expresses the sum of the internal $\mathbf{f}_i$ and external $\mathbf{f}_e$ generalized forces. To solve this set of nonlinear equations an incremental equation is required which can be written, according to the Newton-Raphson solution technique, as

$$\frac{\partial\boldsymbol{\psi}}{\partial\mathbf{d}}\Delta\mathbf{d} = \mathbf{k}\,\Delta\mathbf{d} = \mathbf{f}_i(\mathbf{d}) - \mathbf{f}_e = -\boldsymbol{\psi}(\mathbf{d}) \tag{19}$$

where

$$\mathbf{k} = \mathbf{k}_N + \mathbf{k}_M + \mathbf{k}_Q = \frac{\partial\mathbf{f}_N}{\partial\mathbf{d}} + \frac{\partial\mathbf{f}_M}{\partial\mathbf{d}} + \frac{\partial\mathbf{f}_Q}{\partial\mathbf{d}} \tag{20}$$

defines the element tangent stiffness matrix and $\Delta\mathbf{d}$ represents the incremental displacement vector. It is worth to be noted that the bending stiffness matrix $\mathbf{k}_M$ can be exactly obtained by one-point Gauss quadrature.

Under the small strain assumption, the quantities e_0 and γ can be rewritten as (Santos, 2015)

$$e_0 = \sqrt{(1+u')^2 + w'^2} - 1 \qquad \gamma = \theta - \mathrm{tg}^{-1}\left(\frac{-w'}{1+u'}\right) \tag{21}$$

or, in view of (13),

$$e_0 = \sqrt{\left(1 + \frac{u_{21}}{L_e}\right)^2 + \left(\frac{w_{21}}{L_e}\right)^2} - 1 \qquad \gamma = \theta_1 - \mathrm{tg}^{-1}\left(\frac{-w_{21}}{L_e + u_{21}}\right) + \frac{\theta_{21}}{L_e}X \tag{22}$$

where $u_{21} = u_2 - u_1$, $w_{21} = w_2 - w_1$ and $\theta_{21} = \theta_2 - \theta_1$. If the constraint $e_0 \to 0$ (or $\gamma \to 0$) is imposed by a particular problem then improper relations between some independent nodal displacements are automatically setting in, giving rise to the membrane (or transverse shear) locking. As demonstrated in the sequel, the Gauss quadrature integration scheme is used to properly alleviate such lockings.

NUMERICAL TESTS

In this section, the element effectiveness is investigated by means of nonlinear flexural problems of cantilevers beams with length $L = 3.2$ m and cross-section area $A = 10^{-2}$ m^2 subjected to one of the following loadings: free end moment M, free end transverse load P. The adopted material is defined by $E = 200$ GPa and $G = 77$ GPa. The value $K = 5/6$ is adopted for the shear correction factor. Herein, the quantities U, W, Θ respectively denote the displacement components $u(L)$, $w(L)$, $\theta(L)$ at the beam tip obtained through finite element modeling, and U_{ex}, W_{ex}, Θ_{ex} stand for the exact values of those components assuming $e_0 = \gamma = 0$ (Mattiasson, 1981).

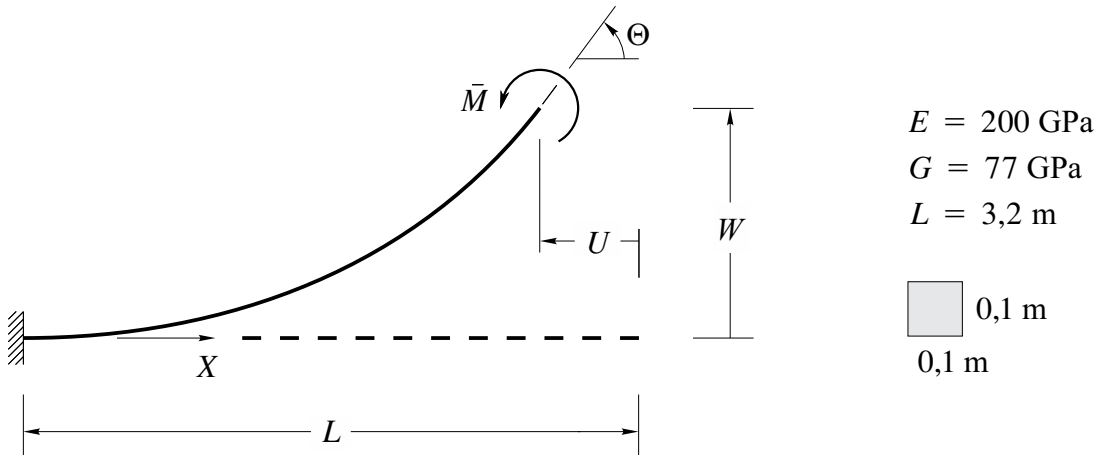

Figure 4 – Cantilever beam with moment.

Cantilever beam with moment at free end

The cantilever beam of Fig. 4 was loaded at the free end by an increasing moment $\overline{M} = ML / 2\pi EI$ till a complete double loop. Departing from a coarse mesh with 5 elements, successive meshes are generated by splitting all elements in the current mesh into smaller ones. Table 1 shows the nondimensional parameters

$$k_u = \frac{U}{U_{ex}} \qquad k_w = \frac{W}{W_{ex}} \qquad k_\theta = \frac{\Theta}{\Theta_{ex}}, \tag{23}$$

the minimum number of increments Inc_{min} to attain the converged solution and the average number of iterations per increment $Iter_{med}$. The values $\overline{M}L / 2\pi EI = 0.5, 1, 1.5$ and 2 correspond to the analytical solutions to reach a half, one, one and a half and two complete loops respectively. As it can be observed, the finer discretization with 50 elements leads to a same precision level than that obtained with 20 elements.

Table 1 – Cantilever beam with moment at free end.

$\overline{M}L / 2\pi EI$	k_u	k_w	k_θ	Inc_{min}	$Iter_{med}$	Mesh
0.5	1,000	1,017	1,000	1	30,0	
1	1,000	1,000	1,000	6	9,2	5 el
1.5	1,000	1,165	1,000	9	9,1	
2	1,000	1,000	1,000	11	14,3	
0.5	1,000	1,004	1,000	3	16,0	
1	1,000	1,000	1,000	6	14,5	10 el
1.5	0,999	1,038	0,999	8	18,9	
2	1,000	1,000	1,000	12	14,0	
0.5	1,000	1,000	1,000	4	11,3	
1	1,000	1,000	1,000	7	12,1	20 el
1.5	1,000	1,009	1,000	10	11,1	
2	1,000	1,000	1,000	13	8,4	
0.5	1,000	1,001	1,000	3	10,3	
1	1,000	1,000	1,000	6	10,2	50 el
1.5	1,000	1,001	1,000	9	10,1	
2	1,000	1,000	1,000	12	10,1	

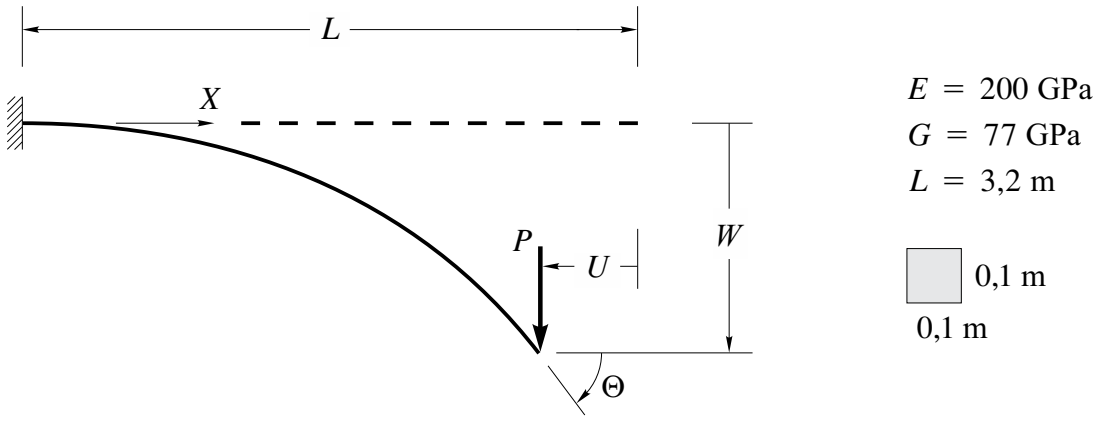

Figure 5 – Cantilever beam with transverse load.

Cantilever beam with transverse load at free end

The beam of Fig. 5 was loaded at the free end by a transverse load $P = 5EI / L^2$. Taking a five element uniform mesh and assigning to the cross-section height the values $h = 0.02, 0.04, 0.06, 0.08$ and 0.1 m one has investigated the influence of reduced integration of $\mathbf{f}_N$, $\mathbf{k}_N$ and $\mathbf{f}_Q$, $\mathbf{k}_Q$ on the accuracy of the finite element models. Figures 6 and 7 compare the k_θ values obtained varying the number of points for the Gauss-Legendre quadrature relative to $\mathbf{f}_N$, $\mathbf{k}_N$ and $\mathbf{f}_Q$, $\mathbf{k}_Q$. As one can observe the more precision involved in the integration process of those quantities the more the membrane and shear locking come to light. According to the numerical tests, evaluation of the involved integrals with just one-point formula properly alleviates such lockings leading to accurate results.

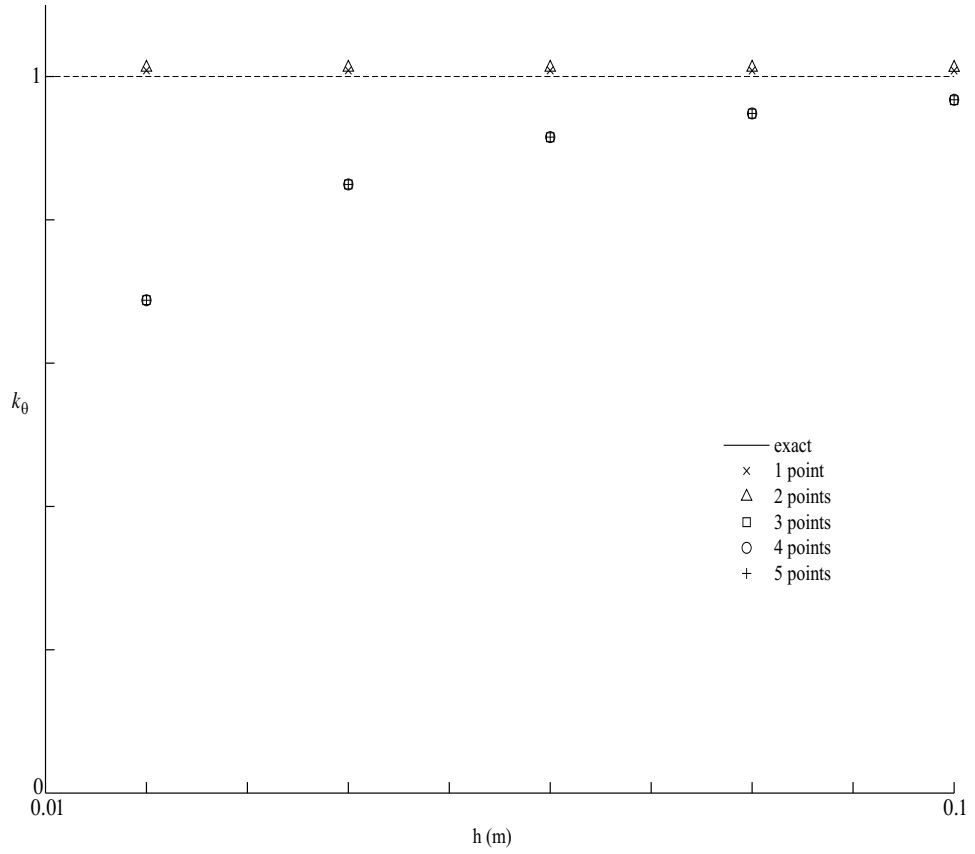

Figure 6 – Values of k_θ considering Gauss-Legendre quadrature with a single point for $\mathbf{f}_M$, $\mathbf{f}_Q$ varying the number of integration points for $\mathbf{f}_N$.

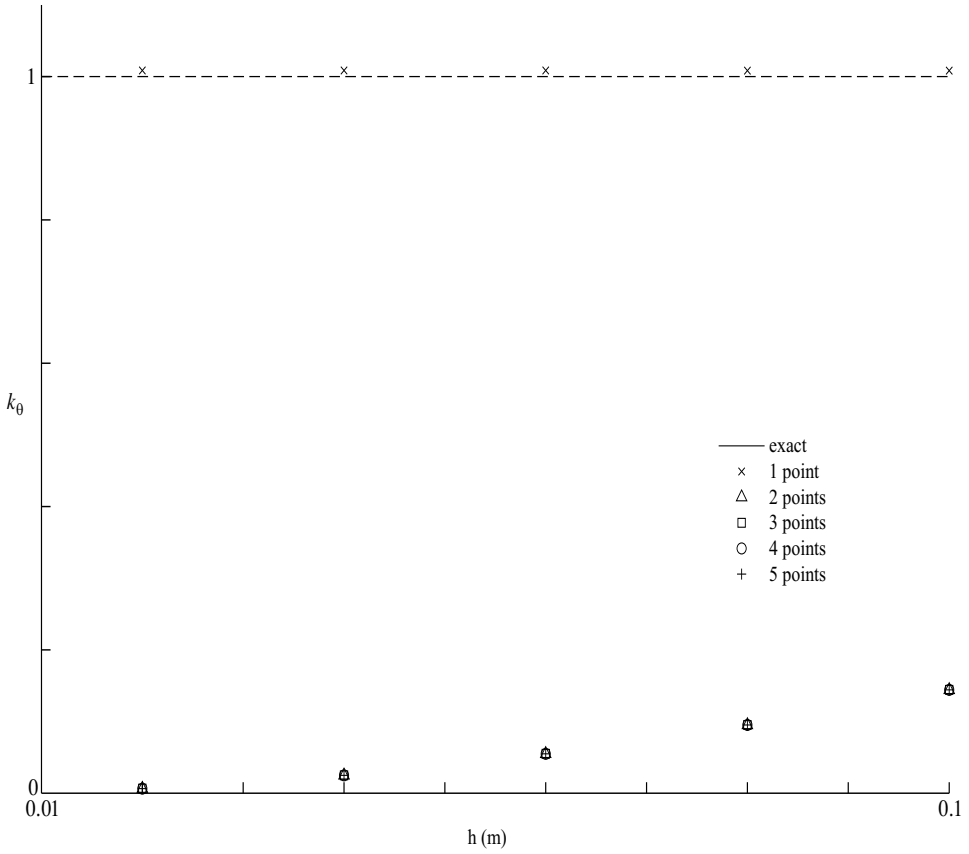

Figure 7 – Values of k_θ considering Gauss-Legendre quadrature with a single point for $\mathbf{f}_M$, $\mathbf{f}_N$ varying the number of integration points for $\mathbf{f}_Q$.

It has been observed that the k_θ values are dependent of the number of integrations points relative to $\mathbf{f}_N$, $\mathbf{f}_Q$ and that the adoption of one-point formula for the Gauss-Legendre quadrature is fundamental to alleviate the membrane and transverse shear lockings. The numerical tests have shown that the multiple point formulas can trigger locking phenomena. According to the scale adopted for the axes in Figs. 6-7, it can be observed that the change of the number of quadrature points has little effect on the k_θ values for multiple point formulas.

CONCLUSION

An intrinsic limitation of the present element is the restriction to small strains. This restriction facilitates the mathematical development of the governing equations being adequate for many structural problems. Based on the examples considered, the following considerations can be drawn with respect to the performance of the proposed consistent strain-gradient-based Timoshenko beam element:

(i) The formulation provides convergence toward exact results with the adoption of just one point integration for the calculation of force vectors and stiffness matrices.

(ii) Multiple point formulas can trigger membrane and transverse shear lockings.

(iii) Precise results are obtained even under coarse meshes for one-point formula.

REFERENCES

Balobanov, V. and Niiranen, J., 2018, "Locking-Free Variational Formulations and Isogeometric Analysis for the Timoshenko Beam Models of Strain Gradient and Classical Elasticity", Computer Methods in Applied Mechanics and Engineering, Vol. 339, pp. 137–159.

Bathe, K.J., 1996, "Finite Element Procedures", Prentice-Hall, Englewood Cliffs.

Beheshti, A., 2016, "Large Deformation Analysis of Strain-Gradient Elastic Beams", Computer and Structures, Vol. 177, pp. 162–175.

Belytschko, T., Liu, W.K., Moran, B. and Elkhodary, K.L., 2014, "Nonlinear Finite Elements for Continua and Structures", 2nd ed., John Wiley, Chichester.

Cescotto, S., Frey, F. and Fonder, G., 1979, "Total and Updated Lagrangian Descriptions in Non-Linear Structural Analysis: A Unified Approach", In Glowinski, R., Rodin, E.Y. and Zeinkiewicz, O.C., eds, Energy Methods in Finite Element Analysis, John Wiley, Chichester, pp. 283–296.

Felippa, C.A, 2014, "Nonlinear Finite Element Methods", http://www.colorado.edu/engineering/cas/course.d/NFEM.d/, Chapter 11.

Kaya, Y. and Dowling, J., 2016, "Application of Timoshenko Beam Theory to the Estimation of Structural Response", Engineering Structures, Vol. 123, pp. 71–76.

Mattiasson, K., 1981, "Numerical Results from Large Deflection Beam and Frame Problems Analysed by Means of Elliptic Integrals", International Journal for Numerical Methods in Engineering, Vol. 17, pp. 145–153.

Reddy, J.N., 2004, "An Introduction to the Finite Element Method", 3rd ed., McGraw-Hill, New York.

Santos, R.R.F., 2015, "Vigas sob Pequenas Deformações mas Grandes Rotações", MSc Thesis, Instituto Tecnológico de Aeronáutica, São Paulo, Brazil.

Zeinkiewicz, O.C., Taylor, R.L. and Zhu, J.Z., 2013, "The Finite Element Method: Its Basis and Fundamentals", 7th ed., Elsevier, Amsterdam.

Zhang, G., Alberdi, R. and Khandelwal, K., 2018, "On the Locking Free Isogeometric Formulations for 3-D Curved Timoshenko Beams", Finite Elements in Analysis and Design, Vol. 143, pp. 46–65.

RESPONSIBILITY NOTICE

The author(s) is (are) the only responsible for the printed material included in this paper.